ResearchGate

See discussions, stats, and author profiles for this publication at: https://www.researchgate.net/publication/236118193

# Elaboration of Hydrogen-Bonded 2D Supramolecular Assemblies on Au(111) From Solutions: Towards NTCDI-Melamine Nanoporous Networks

**ARTICLE** *in* THE JOURNAL OF PHYSICAL CHEMISTRY C · JANUARY 2013

Impact Factor: 4.77 · DOI: 10.1021/jp311356e

CITATIONS
6

READS
60

**8 AUTHORS**, INCLUDING:

Nicolas Battaglini
Paris Diderot University
**33** PUBLICATIONS **264** CITATIONS
SEE PROFILE

Mahamadou Seydou
Paris Diderot University
**42** PUBLICATIONS **149** CITATIONS
SEE PROFILE

Boubakar Diawara
MINES ParisTech
**42** PUBLICATIONS **344** CITATIONS
SEE PROFILE

P. Lang
French National Centre for Scientific Research
**81** PUBLICATIONS **1,810** CITATIONS
SEE PROFILE

Available from: P. Lang
Retrieved on: 02 February 2016

THE JOURNAL OF PHYSICAL CHEMISTRY C

Article

pubs.acs.org/JPCC

# Elaboration of Hydrogen-Bonded 2D Supramolecular Assemblies on Au(111) From Solutions: Toward Naphthalene Tetracarboxylic Diimide–Melamine Nanoporous Networks

J. Teyssandier,[†] N. Battaglini,[†] M. Seydou,[†] G. Anquetin,[†] B. Diawara,[‡] X. Sun,[†] F. Maurel,[†] and P. Lang*[,†]

[†]Univ Paris Diderot, Sorbonne Paris Cité, ITODYS, UMR 7086 CNRS, 15 rue J-A de Baïf, 75205 Paris Cedex 13, France

[‡]Département Moissan FR 3203 CNRS-ENSCP Chime Paristech, 11 rue Pierre et Marie Curie 75005 Paris, France

**ABSTRACT:** Melamine and naphthalene tetracarboxylic diimide (NTCDI) supramolecular assemblies have been elaborated by a solution-based approach on Au(111) and studied by scanning tunneling microscopy (STM). We discuss the role of $\pi$-oligomers and H-oligomers in the mechanism of the network formation. Whereas the role of the first seems negligible, thermodynamical considerations establish the key role of the H-oligomers in the network extension in relation with the solvent nature. Density functional theory (DFT) calculations on the networks support the experimental structures. We discuss the influence and advantages of the solution method on the assemblies comparatively to ultrahigh vacuum (UHV) conditions. The NTCDI–melamine network exhibits a honeycomb structure which is obtained for the first time on the Au(111) substrate. The supramolecular mixed network is remarkably robust due to the stabilization from the triple hydrogen bonds established between the neighboring NTCDI and melamine molecules.

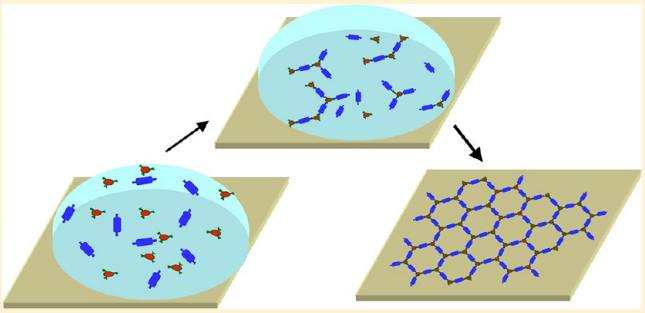

## INTRODUCTION

Following a bottom-up strategy, supramolecular chemistry on surfaces provides a powerful and flexible way to achieve extended molecular patterns on the nanometer scale. Many organic molecules are able to self-organize into 2D networks when deposited on inorganic surfaces (especially Au and HOPG).[1] The supramolecular patterns can be engineered through the design of molecular building blocks. Supramolecular networks have been achieved either through directional noncovalent interactions such as hydrogen bonding,[2] van der Waals interactions,[3] $\pi-\pi$ bonding,[4] and metal coordination[5] or through covalent bonds[6] between single blocks. Moreover, the ability of some molecular systems to form porous 2D structures is of the highest interest as they can be employed as host templates for functional species, giving rise to a supramolecular network with new functionalities.[1,3,4,7] Two main techniques have been applied to develop such systems in the past decade: vapor deposition in ultrahigh vacuum (UHV) and adsorption in solution observed by scanning tunneling microscopy (STM) at the liquid–solid interface. More recently, it has been shown that supramolecular assemblies could be elaborated from solutions (by drop coating or dip coating).[8] In this case, the simplicity of sample preparation and the high stability of the network in a liquid or electrochemical environment make it particularly promising for developing host–guest systems.

The formation of well-ordered molecular templates evaporated in UHV is usually due to a balance between molecule–molecule and molecule–substrate interactions. However, with systems prepared from solution, surface–solvent and molecule–solvent interdependence also have to be taken into account.

Good examples of well-organized arrangements of perylene tetracarboxylic diimide (PTCDI) and melamine (i.e., 1,3,5-triazine-2,4,6-triamine) are obtained by vacuum evaporation either on Ag–Si[2a] or Au[9] or on Au[8a] by the codeposition of the two molecules from solution. In both cases, the supramolecular assembly has a honeycomb structure. Each melamine is linked to three PTCDI molecules through triple hydrogen bonds, and the binding groups are imide, C═O–NH–C═O (ID), and iminodiamine, –NH–C═N–C–NH– (INDA).[10] However, networks made from solution exist in only one crystalline form, and they extend over larger areas than those made under UHV conditions. In the latter case, both dense and porous phases are observed.

Having the same symmetry and the same complementary binding blocks (ID-INDA), naphthalene tetracarboxylic diimide (NTCDI) and melamine networks have also been made by vacuum evaporation on Ag–Si[11] with several dense structures or at the solid–liquid interface on HOPG[12] with only the honeycomb pattern. In the latter case, the pores are smaller. Consequently, the introduction of different spacers between the linking groups makes it possible to tune the pore size to trap

**Received:** November 16, 2012
**Revised:** January 17, 2013
**Published:** January 17, 2013

 © 2013 American Chemical Society  dx.doi.org/10.1021/jp311356e | J. Phys. Chem. C 2013, 117, 8737–8745

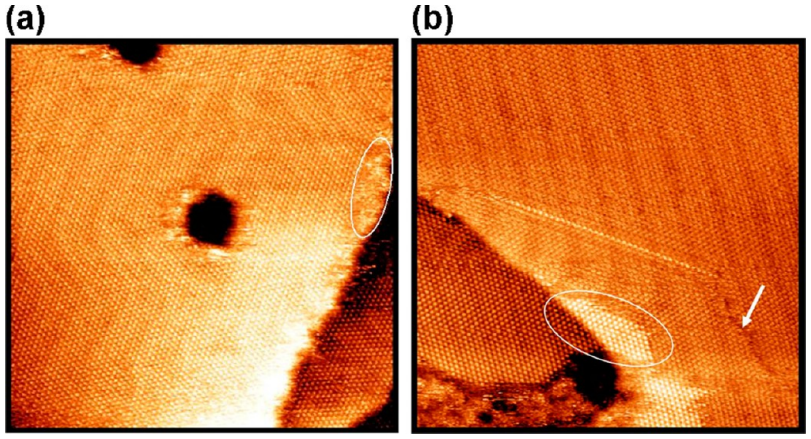


**Figure 1.** Typical STM images (60 nm × 60 nm) of NTCDI assemblies obtained from 1,4-butanediol (left, a) and DMF (right, b).

size-variable guest entities and to control the number of guest molecules per cavity.

In this article, we address the supramolecular organization of NTCDI, melamine, and mixed networks on Au(111), all elaborated via the drop-coating approach.

Unimolecular networks prepared by vapor-phase deposition under vacuum include the close-packed assembly of NTCDI on Ag−Si[13] and Au(111) surfaces.[14] Again, several structures, with either parallel[14a] or tilted[13,14b] molecules, coexist. Melamine networks have been observed either under vacuum[15] or after deposition from solution under ambient conditions.[8b,16]

Here we analyze by STM the crystalline arrangement of 2D networks of these systems elaborated by the drop-coating method on Au(111). The choice of the solvent ensures long-range order of the networks. DFT calculations agree with the stable assemblies observed experimentally.

## EXPERIMENTAL SECTION

Au(111) on mica (Phasis, Geneva, Switzerland), with thickness typically around 200 nm, was chosen as the substrate.

To avoid any organic contamination, the substrates were thoroughly rinsed in pure ethanol and rapidly hydrogen-flamed just before use. After this treatment, STM images exhibit large atomically flat Au(111) terraces (typical width: 200 nm) where herringbone reconstruction is observed.

NTCDI was synthesized by the imidization of naphthalene tetracarboxylic dianhydride (NTCDA, Alfa Aesar, purity 97%) in the presence of $NH_4OH$ at room temperature, using the procedure of Sotiriou-Leventis and Mao.[17]

Melamine (Fluka, purity ≥99%) was used as received. The solvents, dimethylformamide (DMF; Alfa Aesar, purity 99.8%), dimethyl sulfoxide (DMSO; Alfa Aesar, purity 99.9%), and 1,4-butanediol (BD; Acros Organics, purity ≥99%), were used without further purification.

Melamine ($C = 1 \times 10^{-4}$ mol $L^{-1}$) was dissolved in ultrapure water (resistivity: 18 MΩ cm) or DMF. Solutions of NTCDI were prepared in 1,4-butanediol ($C = 1.5 \times 10^{-4}$ mol $L^{-1}$, saturated), DMF (from $1 \times 10^{-4}$ to $4 \times 10^{-4}$ mol $L^{-1}$), or DMSO (from $1 \times 10^{-4}$ to $4 \times 10^{-4}$ mol $L^{-1}$).

The drop-coating method consists of heating separately the solution and the substrate on a hot plate. For melamine, the substrate and the solution were both heated at 90 °C. For NTCDI, the substrate was heated at 170 °C; the solutions in BD and DMSO were heated at 170 °C; and the solution in DMF was heated at 153 °C. Then, one 20 μL droplet of solution was deposited on the Au(111) surface. The substrate temperature was maintained until the solvent was completely evaporated.

For bimolecular NTCDI−melamine networks, two 10 μL droplets of preheated solutions were directly mixed on the gold surface (kept at 90 °C on a hot plate): one droplet of saturated NTCDI in BD at 170 °C ($1.5 \times 10^{-4}$ mol $L^{-1}$) and one droplet of melamine in water at 90 °C. The molecular ratio on the surface is then 3:2 in favor of NTCDI.

STM was performed in the constant current mode under ambient conditions with a Multimode 8 STM head monitored by Nanoscope V electronics (Digital Instruments, USA). Bias voltage and set-point current are as follows: for NTCDI, in the range 200−300 mV and 100−300 pA, for melamine, 100−150 mV and 50−150 pA, and in the case of the mixed network, around 200−300 mV and 150−250 pA. STM data were analyzed with the free WsXm software (Nanotec Electronica, Spain).[18]

Full optimization of possible configurations of NTCDI tetramers was performed by DFT calculation with Gaussian 03 at the B3LYP/6-31G*[19] level of theory, and energies were corrected for the Basis Set Superposition Error (BSSE). Periodic models of monolayers were built using Modelview software.[20] The Vienna Ab-initio Simulations Package (VASP)[21] was used to optimize the latter structure and to compute formation energies of the molecules and their assemblies, excluding any charge transfer with the surface. The geometry and lattice parameters were relaxed in the calculation. VASP performed an iterative solution of the Khon−Sham equations of the density functional theory (DFT) using an augmented plane-wave (PAW) basis set to describe ion−core interaction. The generalized gradient approximation (GGA) method was used to solve the Khon−Sham equations.[22] The convergence of the plane-wave expansion was obtained with a cutoff of 500 eV. The GGA was used with the functional of Perdew−Burke−Ernzerhof (PBE). The Brillouin zone integration in the reciprocal space was performed with a Monkhorst−Pack grid.[23] The sampling in the Brillouin zone was performed on a grid of 3 × 3 × 1 k-points for 2D networks. For monomers and clusters, periodic calculations are performed in vacuum by putting them in a box such that the distance between molecules in neighboring cells is 15 Å. A k-point grid of (1 × 1 × 1) was used. The dispersion contribution was added by using the DFT-D approach proposed recently by Grimme et al.[24]


dx.doi.org/10.1021/jp311356e | J. Phys. Chem. C 2013, 117, 8737−8745

## RESULTS AND DISCUSSION

**1. NTCDI Self-Assemblies.** The nature of the solvent plays an important role in the lateral extension of NTCDI networks formed in BD, DMSO, and DMF. To limit contamination, STM investigations were performed just after completion of the drop-coating process. Figure 1 shows two typical STM images of NTCDI monolayers on Au(111) from BD (Figure 1a) and DMF (Figure 1b) solutions, respectively. The NTCDI networks from DMSO are similar to those from DMF (results not shown). In both cases, the STM images reveal that the highly ordered domains of NTCDI extend over almost the entire gold surface. Nevertheless, small liquid-phase sectors can be found near step edges (highlighted by the circle in Figure 1a). A single layer of NTCDI is generally observed, with occasional brighter islands corresponding to the nucleation of the second layer (highlighted by the circle in Figure 1b). The arrow in Figure 1b points out a grain boundary between two crystalline domains of NTCDI prepared in DMF.

Some discrepancies related to the domain size and the density of grain boundaries were observed between self-assemblies made from BD and those from DMF or DMSO, for solutions of similar concentration. Our STM data show that the average size of NTCDI crystalline domains increases when DMSO is replaced by DMF and when DMF is replaced by BD. With the latter solvent, we never observe grain boundaries on the STM images, which are up to 400 nm × 400 nm in size, and the size of the domains is limited only by that of the terraces. In the following, we investigate more thoroughly the mechanism that could explain the relationship between the solvent properties and the extension of the networks. UV−visible spectroscopy shows that the limit of solubility for NTCDI at room temperature is $3 \times 10^{-5}$ mol $L^{-1}$ in BD, $4.5 \times 10^{-4}$ mol $L^{-1}$ in DMF, and $1.7 \times 10^{-3}$ mol $L^{-1}$ in DMSO. [The extinction coefficient of the free monomer ($\varepsilon_{379nm} = 1.85 \times 10^4$ L $mol^{-1}$ $cm^{-1}$; $\varepsilon_{360nm} = 1.51 \times 10^4$ L $mol^{-1}$ $cm^{-1}$; $\varepsilon_{342nm} = 0.95 \times 10^4$ L $mol^{-1}$ $cm^{-1}$) has been measured in DMSO (it is assumed to be independent from the solvent) and is in good agreement with the literature for naphthalene derivatives.[25]] Moreover, the solubility of NTCDI increases when the solution is heated. We conclude, depending on the choice of the solvents, that the greater the NTCDI solubility, the smaller the domain size. Interactions between the NTCDI and the solvent molecules clearly influence the formation of organized supramolecular networks.

Unlike supramolecular systems elaborated in vacuum, where the organization process addresses only adsorbed species, the pattern of molecular networks made from solution is the result of a sequence of chemical reactions that take place either in solution or on the surface, or both (see Scheme 1). Indeed, solvated monomers can aggregate into $\pi$-oligomers (i.e., bunches of molecules interacting through $\pi$-stacking).[25] The monomer is likely also to be in equilibrium with a hydrogen-bonded H-dimer. Some H-oligomers can also be generated, as a preliminary step to the formation of the NTCDI network. The latter reactions can also take place on the surface once a monomer or a H-oligomer is adsorbed on the gold substrate. Obviously the relative solvation and adsorption energies and intermolecular interactions of NTCDI and its oligomers determine the true sequence.

To determine the composition of the solutions prior to formation of the network, UV−visible spectroscopy was performed on NTCDI solutions heated at about 150 °C.

**Scheme 1. Sequence of Chemical Reactions Occurring in Solution and on the Surface Leading to 2D Supramolecular Assemblies of NTCDI**

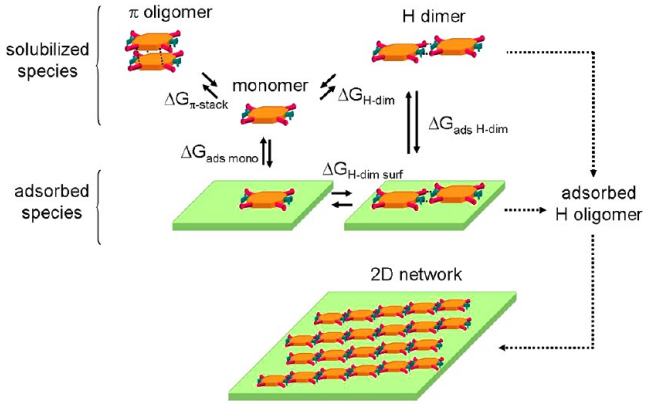


Figure 2 shows typical absorption spectra of NTCDI in BD, DMF, and DMSO. The free monomers exhibit a typical vibronic structure between 300 and 400 nm.[25,26] Depending on the solvent, there is a broad absorption band beyond 400 nm (see inset in Figure 2). This band is the signature of the presence of $\pi$-oligomers in the solution and compares well with many other perylene diimide derivatives.[25,26] Recent calculations[27] and experimental data[28] have confirmed the important redshift due to the aggregation.[27] The concentration of $\pi$-aggregated molecules is the largest in BD and the lowest in DMSO. Ratios between absorption band intensities of $\pi$-oligomers and free monomers allow the evaluation of the concentration of such species as a function of the solvent. Table 1 summarizes our results.

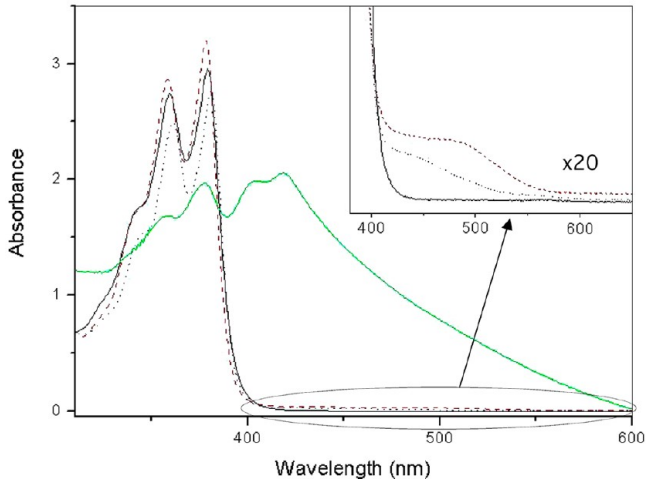


**Figure 2.** UV−visible spectra of NTCDI solutions in 1,4-butanediol at room temperature (green line, magnified 5 times), in BD at 150 °C (red dashed line), in DMF at RT (blue dotted line), and in DMSO (black line) at RT.

It is noteworthy that the number of $\pi$-aggregated molecules is greater for BD, which is the solvent that leads to the more extended NTCDI networks. Moreover, under our experimental conditions, the concentration of free monomers is roughly identical for the three solvents. Therefore, this shows that the presence of $\pi$-oligomers (soluble or insoluble) hinders neither


dx.doi.org/10.1021/jp311356e | J. Phys. Chem. C 2013, 117, 8737−8745

**Table 1. Concentrations of Free and $\pi$-Aggregated NTCDI Species Estimated by UV−Visible Spectroscopy of NTCDI Solutions in Three Solvents (at ca. 150 °C) Assuming an Identical Absorption Coefficient for the Two Species[29]**

| | free monomer conc. | $\pi$-oligomer conc. |
|---|---|---|
| BD (sat. solution) | $\approx 10^{-4}$ | $\approx 4 \times 10^{-6}$ |
| DMF (unsat. solution) | $\approx 10^{-4}$ | $<1 \times 10^{-6}$ |
| DMSO (unsat. solution) | $\approx 10^{-4}$ | $<3 \times 10^{-7}$ |

the adsorption of NTCDI nor the formation of assemblies through H-bonding but limits the solubility of NTCDI.

Hunter[30] has expressed the variation of the free enthalpy $\Delta G_{\text{H-dim}}$ of the reaction of H-dimerization by hydrogen bonding between two molecules M at the expense of the solvation by a solvent S. These calculations are based on hydrogen-bonding interactions of molecules via their chemical functions and their H-donor and H-acceptor characters. The equilibrium can be written

$$M_S + M_S \overset{K_{H-dim}}{\rightleftharpoons} M\cdots M + S\cdots S \quad (1)$$

where $M_S$ represents a solvated NTCDI unit. Table 2 gives $\Delta G_{\text{H-dim}}$ for the reaction of H-dimerization calculated according to Hunter (eq 11 and corresponding data taken in Table 3 of Hunter's publication).[30]

**Table 2. Estimations of the Free Enthalpy of H-Dimer Formation (Equation 1) and the Corresponding Equilibrium Constant in the Three Solvents at Room Temperature**

| | $\Delta G_{\text{H-dim}}$ (kJ/mol) | $K_{\text{H-dim}}$ |
|---|---|---|
| BD | −0.5 | 1.2 |
| DMF | 6 | 0.10 |
| DMSO | 13 | 0.005 |

BD appears to be the most favorable solvent to the formation of H-dimers in solution, with roughly 12 times more H-dimers than with DMF and 240 times more than with DMSO. One would expect the same tendency for longer oligomers in solution, i.e., a greater proportion of H-oligomers in BD.

It is noteworthy that compared to the adsorption energy of NTCDI on gold the previous calculated free enthalpies of H-dimer formation are low.[8a,31] However, they show qualitatively which solvent is the most appropriate for the formation of H-dimer/oligomers in solution. Obviously, an increase in the size of the H-oligomer leads to the decrease in its solvation. Besides, the free enthalpy of adsorption of the solvents on gold (i.e., physisorption) is relatively low compared to the energy of adsorption of NTCDI.[31] This suggests that the adsorption of H-oligomers should be favored as soon as a H-oligomer reaches a critical size. This critical size may possibly be reduced to a single monomer, depending on the solvent. Compared to the sequence of reactions followed in solution, the growth of H-oligomers between adsorbed species should be described with similar energy considerations. Indeed, since the energetic considerations originate from interactions between the functions taken individually, the following steps, such as formation/precipitation/growth of the dimers, trimers, ..., should obey the same rule. In other terms, a strong H-interaction developed between the monomers at the expense of solvation will be found with oligomers whether they are adsorbed or not. The formation of an adsorbed NTCDI dimer from a solvated monomer or solvated H-dimer (Scheme 1) indeed occurs with a loss of solvation, the latter being more important at the edge of the H-dimer, where the imide moieties are still available.

In conclusion, some simple energetic considerations on solvation suggest that the formation of H-oligomers, adsorbed or not, is a key step for the building of extended supramolecular 2D networks from solution. The formation of extended $\pi$-oligomers does not interfere with the formation of the network but limits the solubility.

The crystalline structure from drop-coating processed NTCDI networks was studied using STM. Figure 3 shows high-resolution STM images of the molecular packing obtained from BD and from DMF, revealing a close-packed assembly of NTCDI molecules. Each NTCDI appears as a bright "rugby ball"-shaped protrusion. The network is nearly defect-free: there are very few molecular vacancies. The NTCDI network appears to be particularly stable insofar as even sonication in dichloromethane does not remove it.

The image from DMF clearly reveals that the molecules adopt herringbone packing and are inclined alternately to one side or the other with respect to the direction of a row of molecules. The Fourier transform characteristic of the crystal lattice structure of the image is shown. The brighter spots correspond to hexagonal packing. Less bright spots in between

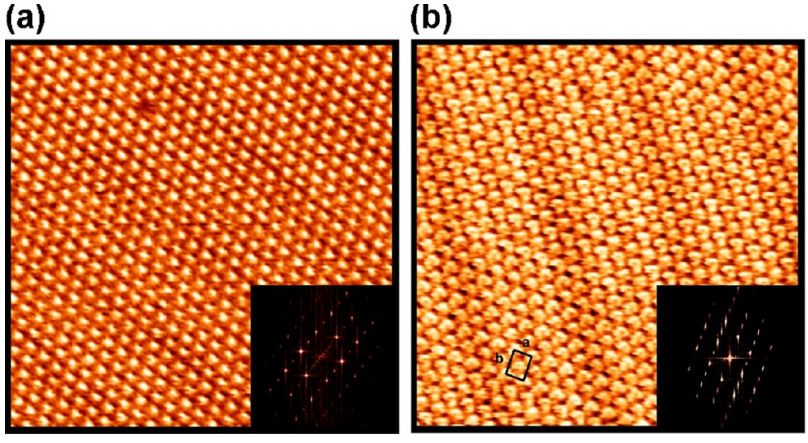


**Figure 3.** High-resolution (20 nm × 20 nm) STM images of NTCDI networks on Au(111) prepared from solutions in BD (left, a) and DMF (right, b). Insets: corresponding Fourier transform patterns.


dx.doi.org/10.1021/jp311356e | J. Phys. Chem. C 2013, 117, 8737−8745

correspond to the superstructure related to the herringbone packing. The unit cell highlighted on the image contains two molecules. Lattice parameters: $a = 0.99 \pm 0.02$ nm; $b = 1.59 \pm 0.07$ nm; $\gamma = 88 \pm 1°$, with an area per molecule of 0.786 nm$^2$.

The molecular orientation of NTCDI from BD (Figure 3, left) is rather difficult to resolve in the real-space STM images. However, the Fourier transform pattern is similar to that obtained for the NTCDI network from DMF. Crystalline lattice parameters are similar for the two solvents, indicating that the solvent has no influence on the local organization of the molecules (STM images from DMSO also lead to the same conclusion). Contrast changes between the two images of Figure 3(a) and (b) are related either to STM tip artifacts or to electronic effects due to different adsorption sites for NTCDI.

Comparing our results with earlier work obtained under different experimental conditions, we notice that the intermolecular spacing along the long axis ($0.99 \pm 0.02$ nm) is very close to those measured by X-ray diffraction in the bulk structure (1.018 nm)[13] and in previous STM experiments (from 0.998 to 1.1 nm).[13,14] Moreover, the herringbone packing observed for NTCDI is consistent with previous observations made for PTCDI assemblies,[32] the perylene group separating the anchoring functions being simply longer than the naphthalene one. However, Ruiz-Osés et al. have indicated that the molecular orientation of NTCDI is not always clearly discernible. They showed an STM image of the NTCDI network on a Au(111) surface, obtained in UHV and interpreted by DFT calculations.[14a] They suggest a network with an oblique lattice unit cell (lattice parameters: $1.10 \times 1.08$ nm$^2$ and $\gamma = 80.08°$) and one molecule per unit cell, where all the molecules have the same orientation.

In a first step, we have estimated the interaction energy of the NTCDI dimer using DFT methods and compared them with themselves and with the literature.[33] Our values are closely related and well aligned with those found previously by MP2 and DFT//M06 methods. Results also show a contribution of the dispersion to the stability of 10 kJ/mol (Table 3).

**Table 3. NTCDI−NTCDI Interaction Energy Computed by Different Methods**

| methods | $E_s$ (kJ/mol) |
|---|---|
| DFT/Gaussian09 (B3LYP/6-31G*) | −38.99 (with BSSE correction) |
| DFT/VASP (PAW-PBE+vdW) | −56.1 (VdW contribution = −10.6) |
| MP2[33] | −41.8 |
| DFT/M06[33] | −43 |

To understand the stability of the two structures (parallel and tilted), we estimated by DFT calculations the energies for both NTCDI structures in the absence of surface. We started with tetramers, denoted in the following by TA for the parallel assembly and TB for the tilted one. Full energy optimization of the two tetramers (see Experimental Section for complete details on the computation) shows that the tilted TB assembly is 10 kJ/mol more stable than TA. On the basis of the tetramers, monolayers (MONA and MONB) were built. Optimized monolayer structures are presented in Figure 4. To simplify the following discussion, we consider a supercell containing two molecules for MONA.

In the parallel structure (i.e., MONA), each NTCDI molecule interacts with two neighbors in the $A_2$ direction, through a couple of strong hydrogen bonds ($d$(N−H···O═C) = 1.70 Å) and with two others in the $A_1$ direction by two pairs of weak hydrogen bonds ($d$(C═O···H−C) = 2.15 Å). In the tilted packing (i.e., MONB), the interaction along the $A_2$ axis is identical to that for MONA. However, along the $A_2$ direction, each NTCDI interacts with four neighbors by weak single hydrogen bonds ($d$(C═O···H−C) = 1.89 and 1.84 Å). The number of hydrogen bonds per molecule is thus the same for MONA and MONB with, however, some differences in length. The lattice parameters (see caption of Figure 4) and area per molecule (i.e., 0.825 nm$^2$) of MONB are in good agreement with our STM results. We calculated the stabilization energies, which are defined as the difference between the total energy per cell embedded in the optimized monolayer and twice the total energy of a monomer (this energy corresponds to a monomer set in a large cell, so that interactions with molecules of other cells are negligible). The stabilization energy of MONA is −153 kJ/mol (−1.59 eV per unit cell), and that of MONB is −168 kJ/mol (−1.74 eV per unit cell).

MONB is very similar to the most stable monolayer structure found for PTCDI (named MON8 by Mura et al.).[32a] The stabilization energy found for MONB is greater than that (corrected for BSSE) of the PTCDI MON8 configuration (−1 eV) and noticeably larger than those published for PTCDA (structure MON8: −0.54 eV and structure MON9: −0.70 eV).[34] Nevertheless, the discrepancy between our calculations and the values reported in the literature can be explained by the fact that we took into account the dispersive van der Waals interactions which provide a supplementary stabilization energy of −52.5 kJ/mol (−0.54 eV). Excluding this contribution, the results are comparable.

MONB is more stable than MONA by 15 kJ/mol. Thus, the drop-coating process leads to only one structure that is the more stable one.

**2. Melamine Self-Assemblies.** The solvent for the elaboration of melamine monolayers by drop coating is ultrapure water or DMF. In both cases, STM images obtained after the evaporation of the solvent show a surface highly covered by ordered melamine networks. The average size of an ordered melamine domain generally extends to around 30 nm. The melamine network is not removed by rinsing in dichloromethane. The high-resolution STM image in Figure 5a shows the typical honeycomb network adopted by melamine blocks, in agreement with previous work.[8b,15] Each molecule appears as a triangular protrusion where the $NH_2$ groups are located at the summits of the triangles.

Figure 5b highlights the pore structure of the molecular assembly with hydrogen bonds. The melamine network has a hexagonal ordering which is stabilized by the formation of strong double hydrogen bonds (NH···N). Unlike melamine monolayers made in UHV,[15b] a unique defect-free hexagonal melamine structure is observed. The experimental lattice parameter ($a = 1.04 \pm 0.03$ nm) is in accordance with previously published results for the melamine honeycomb network[8b,9,15] and with our calculations ($a = 1.04$ nm) performed in the absence of a surface. It suggests that the influence of the substrate is not observable. We find a stabilization energy of −162 kJ/mol (−1.68 eV per unit cell). The stabilization energy found by Silly et al. is −1.29 eV per unit cell. The discrepancy with our values arises probably from the fact that van der Waals interactions (−0.59 eV/−57.3 kJ/mol) were not taken into account in the previous work.

We thus conclude that, also for melamine networks, the drop coating method gives only one structure, and this structure is the most stable observed experimentally.


dx.doi.org/10.1021/jp311356e | J. Phys. Chem. C 2013, 117, 8737−8745

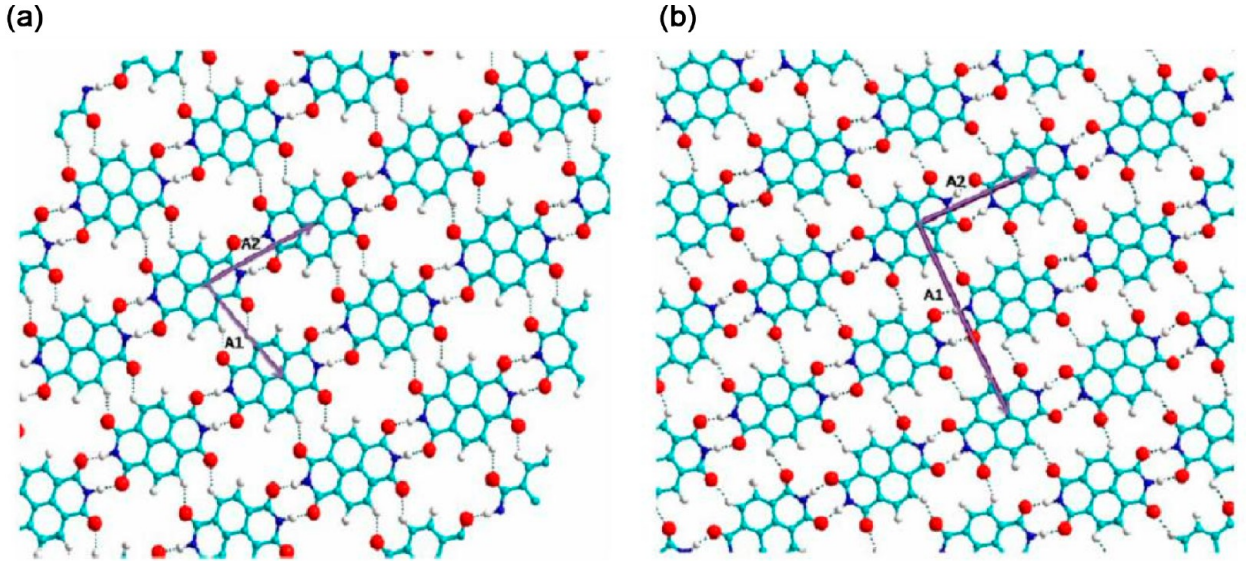


**Figure 4.** Optimized structures for the NTCDI monolayer. (a) Parallel structure (MONA); lattice parameters: $A_1$ = 0.888 nm, $A_2$ = 1.005 nm, $\gamma$ = 75.72°. (b) Canted structure (MONB); lattice parameters: $A_1$ = 1.641 nm, $A_2$ = 1.006 nm, $\gamma$ = 88.88°.

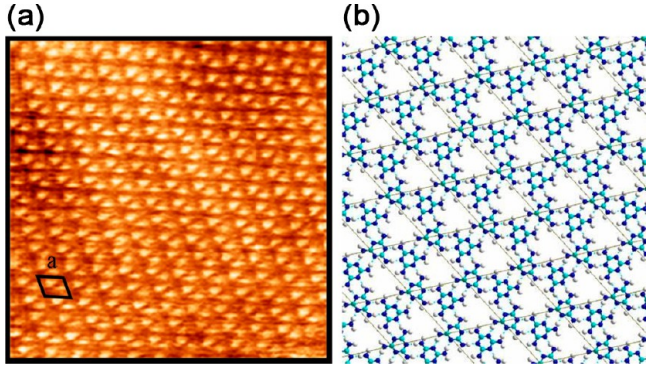


**Figure 5.** (a) STM image of the melamine honeycomb network on Au(111) (10 × 10 nm); magnified image in inset. (b) Calculated structure of melamine porous network motif showing hydrogen bond interactions between the building blocks.

**3. Bicomponent Molecular Self-Assemblies.** Mixed NTCDI−melamine networks were elaborated by drop coating on Au(111). On the basis of the previous experimental findings that melamine networks can be formed simply in water and that NTCDI is better organized when prepared from BD (DMF and DMSO interfere more with the self-assembly process), solutions of melamine in water and NTCDI in BD (saturated) were used for preparing bicomponent NTCDI−melamine networks. As with the NTCDI network, the presence of $\pi$-oligomers does not hinder the formation of the mixed network. After solvent evaporation, STM results show that close to 80% of the surface is covered by the organized NTCDI−melamine networks (Figure 6a). The largest domains can reach a size of approximately 100 nm. The network is notably stable since we succeeded in building a host−guest system with 1-adamantanethiol in ethanol (not shown).

The local arrangement of the network as seen from the high-resolution STM image is shown in Figure 6b. Melamine molecules appear darker under STM due to the lower density of states. NTCDI and melamine molecules adopt a honeycomb structure. Each melamine molecule is connected through triple hydrogen bonds (i.e., two NH···O and one NH···N) to three NTCDI blocks, as shown by the model in Figure 6c. This result is consistent with previous reports on PTCDI−melamine and NTCDI−melamine networks[2a,8a,12] formed under different conditions. The experimental unit cell parameter of the honeycomb is 2.5 ± 0.2 nm, and the pore diameter is 1.7 ± 0.2 nm, which agrees well with the values of Palma et al. (2.8 ± 0.2 and 1.6 nm, respectively)[12] and our calculated values (2.6 and 1.9 nm). The main defects of the network are molecular vacancies, stacking fault lines, and filled pores (probably with one NTCDI molecule). It is noteworthy that whatever the domains considered we observe two distinct orientations between organized domains (highlighted for instance by the arrows in Figure 6). The mismatch angle between molecular domains is 10° (±2°). This specific feature has not been reported before. We assume that NTCDI−melamine molecular layers grow epitaxially on the Au(111) surface: as shown in Figure 6d, the mismatch can be explained with a $(\sqrt{73} \times \sqrt{73})$R5.8° superlattice of the NTCDI−melamine network. Thus, we find a lattice parameter of 2.46 nm very close to the experimental value of 2.5 nm and an angle of 11.6°, also within experimental error. The theoretical value calculated without taking into account the surface (111) gives 2.6 nm, a significantly higher value than the value of the model with the surface. This difference of 5% may be accounted for by the force applied to the network to be related epitaxially to the Au(111) surface. Let us notice that we could also take a gold atom more in the gold mesh and then find a $(\sqrt{91} \times \sqrt{91})$ R5.4° superlattice. That would give 2.74 nm for the lattice parameter—within experimental error—with a lengthening of the mesh of organic network of 5%.

We also note clearly on the high-resolution image inset that only molecules NTCDI appear, which is related to the density of state of the two molecules. Melamine molecules are still present in every empty space.

The stabilization energy of the network is −5.19 eV (−500.1 kJ/mol) per unit cell (the unit cell consists of two melamine molecules and three NTCDI molecules). Thus, for a given number of melamine and NTCDI molecules, their organization in a mixed network is more favorable by 0.9 eV than those in two distinct homomolecular networks. We can compare the


dx.doi.org/10.1021/jp311356e | J. Phys. Chem. C 2013, 117, 8737−8745

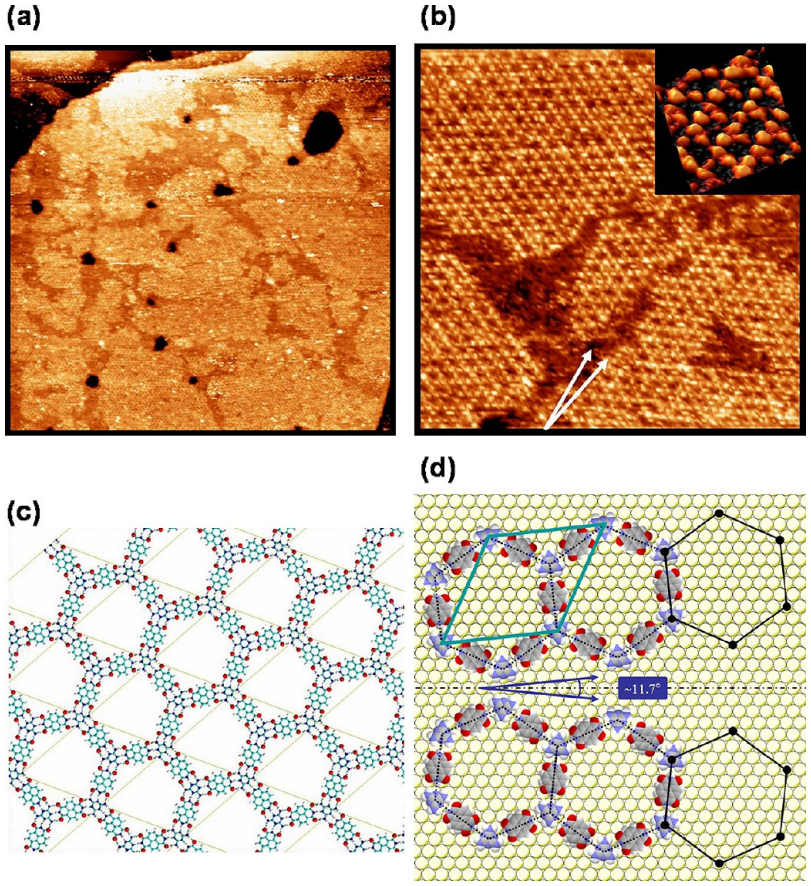


**Figure 6.** (a) Large-scale STM image (250 nm × 250 nm) of the NTCDI−melamine network on Au(111). (b) High-resolution STM image (60 nm × 60 nm; inset: 8 nm × 8 nm). (c) Optimized structure of the mixed network and its primitive cell exhibiting the triple hydrogen bonds between the molecules. (d) The two observed ($\sqrt{73} \times \sqrt{73}$)R5.8° superlattices of the NTCDI−melamine network formed epitaxially on Au(111).

above energy reduced to the melamine−NTCDI interaction (3 hydrogen bonds), i.e., $E_{dimixt} \approx 95$ kJ, to the corresponding ones of the literature: we find relatively closed values with $E_{dimixt}$ = 105 or 117 kJ calculated for a pore and by MP2 and M06 methods, respectively.[12] In the case of the PTCDI−melamine network, a weaker value (−4.40 eV) has been calculated for this energy.[10] The difference comes from the fact that the van der Waals interactions (−1.18 eV/−114.8 kJ/mol) were not taken into account. Once again, only one crystalline structure (the more stable one) is obtained by the drop-coating approach.

## CONCLUSION

We have elaborated supramolecular assemblies of NTCDI, melamine, and mixed NTCDI−melamine molecular networks on Au(111) by means of hydrogen bonding between molecular building blocks. We have shown that these networks can be formed through solution processing, namely, "drop coating". The melamine, NTCDI, and NTCDI−melamine networks remain stable on the Au(111) surface despite solvent evaporation or rinsing in dichloromethane, and the mixed one can then be employed as a host template. The choice of the solvent has turned out to be a critical factor in the process since it affects the molecular assembly process. For NTCDI, the solvent modifies the spatial extension of the crystalline domains (1,4-butanediol being the solvent allowing the formation of the most extended domains). We have correlated the domain size and the ability of the solvent to promote H-oligomer formation either in solution or on the surface. On the other hand, the formation of $\pi$-oligomers does not interfere with molecular assembly. For both NTCDI and melamine networks, STM images reveal that the solvent does not affect the local molecular order. We achieved a bicomponent NTCDI−melamine network with a honeycomb structure, in which one melamine is strongly connected through three triple hydrogen bonds to three adjacent NTCDI molecules, via the ID−INDA sequence. Thanks to very strong bonds, the organization of melamine and NTCDI molecules in a mixed network is energetically more favorable than those of the two homomolecular networks, as proved by DFT calculations. Moreover, the NTCDI−melamine network grows epitaxially on the Au(111) surface. This network has the same structure as the well-known PTCDI−melamine system,[2a,8a] whereas the pore size is roughly two times lower.

The drop-coating method gives rise to only one crystalline structure, that which has been shown by DFT calculations to be the most stable. The coverage of the networks is higher than what is obtained under UHV conditions. In a next step, we plan to adsorb an electroactive thiol in the pores and to probe the electrochemical properties of the confined molecules.

## AUTHOR INFORMATION

### Corresponding Author

*E-mail: lang@univ-paris-diderot.fr.

### Notes

The authors declare no competing financial interest.

## ■ ACKNOWLEDGMENTS

We would like to thank John Lomas for rereading the article in English

## ■ REFERENCES

(1) Kudernac, T.; Lei, S.; Elemans, J. A. A. W.; De Feyter, S. Two-Dimensional Supramolecular Self-Assembly: Nanoporous Networks on Surfaces. *Chem. Soc. Rev.* **2009**, *38* (2), 402−421.

(2) (a) Theobald, J. A.; Oxtoby, N. S.; Phillips, M. A.; Champness, N. R.; Beton, P. H. Controlling Molecular Deposition and Layer Structure with Supramolecular Surface Assemblies. *Nature* **2003**, *424* (6952), 1029−1031. (b) Slater, A. G.; Beton, P. H.; Champness, N. R. Two-Dimensional Supramolecular Chemistry on Surfaces. *Chem. Sci.* **2011**, *2* (8), 1440−1448.

(3) Schull, G.; Douillard, L.; Fiorini-Debuisschert, C.; Charra, F.; Mathevet, F.; Kreher, D.; Attias, A. J. Single-Molecule Dynamics in a Self-Assembled 2D Molecular Sieve. *Nano Lett.* **2006**, *6* (7), 1360−1363.

(4) (a) Mena-Osteritz, E.; Bäuerle, P. Complexation of C60 on a Cyclothiophene Monolayer Template. *Adv. Mater.* **2006**, *18* (4), 447−451. (b) Schenning, A. P. H. J.; Meijer, E. Supramolecular Electronics; Nanowires from Self-Assembled π-Conjugated Systems. *Chem. Commun.* **2005**, *26*, 3245−3258.

(5) Stepanow, S.; Lingenfelder, M.; Dmitriev, A.; Spillmann, H.; Delvigne, E.; Lin, N.; Deng, X.; Cai, C.; Barth, J. V.; Kern, K. Steering Molecular Organization and Host−Guest Interactions Using Two-Dimensional Nanoporous Coordination Systems. *Nature Mater.* **2004**, *3* (4), 229−233.

(6) (a) Zwaneveld, N. A. A.; Pawlak, R.; Abel, M.; Catalin, D.; Gigmes, D.; Bertin, D.; Porte, L. Organized Formation of 2D Extended Covalent Organic Frameworks at Surfaces. *J. Am. Chem. Soc.* **2008**, *130* (21), 6678−6679. (b) Abel, M.; Clair, S.; Ourdjini, O.; Mossoyan, M.; Porte, L. Single Layer of Polymeric Fe-Phthalocyanine: An Organometallic Sheet on Metal and Thin Insulating Film. *J. Am. Chem. Soc.* **2011**, *133*, 1203−1205.

(7) Furukawa, S.; Tahara, K.; De Schryver, F. C.; Van der Auweraer, M.; Tobe, Y.; De Feyter, S. Structural Transformation of a Two-Dimensional Molecular Network in Response to Selective Guest Inclusion. *Angew. Chem., Int. Ed.* **2007**, *119* (16), 2889−2892.

(8) (a) Madueno, R.; Räisänen, M. T.; Silien, C.; Buck, M. Functionalizing Hydrogen-Bonded Surface Networks with Self-Assembled Monolayers. *Nature* **2008**, *454* (7204), 618−621. (b) Zhang, H. M.; Xie, Z. X.; Long, L. S.; Zhong, H. P.; Zhao, W.; Mao, B. W.; Xu, X.; Zheng, L. S. One-Step Preparation of Large-Scale Self-Assembled Monolayers of Cyanuric Acid and Melamine Supramolecular Species on Au (111) Surfaces. *J. Phys. Chem. C* **2008**, *112*, 4209−4218.

(9) Perdigão, L.; Perkins, E.; Ma, J.; Staniec, P.; Rogers, B.; Champness, N.; Beton, P. Bimolecular Networks and Supramolecular Traps on Au (111). *J. Phys. Chem. B* **2006**, *110* (25), 12539−12542.

(10) Sassi, M.; Oison, V.; Debierre, J.-M. First Principle Study of a Bimolecular Thin Film on Ag(111) Surface. *Surf. Sci.* **2008**, *602* (17), 2856−2862.

(11) Perdigão, L. M. A.; Fontes, G. N.; Rogers, B. L.; Oxtoby, N. S.; Goretzki, G.; Champness, N. R.; Beton, P. H. Coadsorbed NTCDI−Melamine Mixed Phases on Ag-Si (111). *Phys. Rev. B* **2007**, *76* (24), 245402.

(12) Palma, C. A.; Bjork, J.; Bonini, M.; Dyer, M. S.; Llanes-Pallas, A.; Bonifazi, D.; Persson, M.; Samori, P. Tailoring Bicomponent Supramolecular Nanoporous Networks: Phase Segregation, Polymorphism, and Glasses at the Solid−Liquid Interface. *J. Am. Chem. Soc.* **2009**, *131* (36), 13062−13071.

(13) Keeling, D.; Oxtoby, N.; Wilson, C.; Humphry, M.; Champness, N.; Beton, P. Assembly and Processing of Hydrogen Bond Induced Supramolecular Nanostructures. *Nano Lett.* **2003**, *3* (1), 9−12.

(14) (a) Ruiz-Osés, M.; Gonzalez-Lakunza, N.; Silanes, I.; Gourdon, A.; Arnau, A.; Ortega, J. Self-assembly of heterogeneous supramolecular structures with uniaxial anisotropy. *J. Phys. Chem. B* **2006**, *110* (51), 25573−25577. (b) Ruiz-Osés, M.; Kampen, T.; González-Lakunza, N.; Silanes, I.; Schmidt-Weber, P. M.; Gourdon, A.; Arnau, A.; Horn, K.; Ortega, J. E. Spectroscopic Fingerprints of Amine and Imide Functional Groups in Self-Assembled Monolayers. *ChemPhysChem* **2007**, *8* (11), 1722−1726.

(15) (a) Xu, W.; Dong, M.; Gersen, H.; Rauls, E.; Vázquez Campos, S.; Crego Calama, M.; Reinhoudt, D. N.; Stensgaard, I.; Laegsgaard, E.; Linderoth, T. R.; Besenbacher, F. Cyanuric Acid and Melamine on Au (111): Structure and Energetics of Hydrogen Bonded Networks. *Small* **2007**, *3* (5), 854−858. (b) Silly, F.; Shaw, A. Q.; Castell, M. R.; Briggs, G. A. D.; Mura, M.; Martsinovich, N.; Kantorovich, L. Melamine Structures on the Au (111) Surface. *J. Phys. Chem. C* **2008**, *112* (30), 11476−11480.

(16) Zhang, H. M.; Pei, Z. K.; Xie, Z. X.; Long, L. S.; Mao, B. W.; Xu, X.; Zheng, L. S. Preparing Self-Assembled Monolayers of Cyanuric Acid and Melamine Complex on HOPG Surfaces. *J. Phy. Chem. C* **2009**, *113* (31), 13940−13946.

(17) Sotiriou-Leventis, C.; Mao, Z. A Facile Synthesis of 2,7-Diazapyrene. *J. Heterocycl. Chem.* **2000**, *37* (6), 1665−1667.

(18) Horcas, I.; Fernandez, R.; Gomez-Rodriguez, J.; Colchero, J.; Gómez-Herrero, J.; Baro, A. WSXM: A Software for Scanning Probe Microscopy and a Tool for Nanotechnology. *Rev. Sci. Instrum.* **2007**, *78*, 013705.

(19) (a) Frisch, M. J. et al. *Gaussian 03*, Revision E.01; Gaussian, Inc.: Wallingford, CT, 2004. (b) Becke, A. D. Density-Functional Thermochemistry. III. The Role of Exact Exchange. *Chem. Phys.* **1993**, *98* (1), 5648−5652. (c) Lee, C.; Yang, W.; Parr, R. G. Development of the Colle−Salvetti Correlation-Energy Formula into a Functional of the Electron Density. *Phys. Rev. B* **1988**, *37* (2), 785.

(20) http://modelview.fr/.

(21) (a) Kresse, G.; Hafner, J. Ab Initio Molecular Dynamics for Liquid Metals. *Phys. Rev. B* **1993**, *47* (1), 558−561. (b) Kresse, G.; Furthmüller, J. Efficiency of Ab-Initio Total Energy Calculations for Metals and Semiconductors Using a Plane-Wave Basis Set. *Comput. Mater. Sci.* **1996**, *6* (1), 15−50.

(22) Perdew, J. P.; Zunger, A. Self-Interaction Correction to Density-Functional Approximations for Many-Electron Systems. *Phys. Rev. B* **1981**, *23* (10), 5048−5079.

(23) Monkhorst, H. J.; Pack, J. D. Special Points for Brillouin-Zone Integrations. *Phys. Rev. B* **1976**, *13* (12), 5188−5192.

(24) Grimme, S.; Antony, J.; Ehrlich, S.; Krieg, H. A Consistent and Accurate Ab Initio Parametrization of Density Functional Dispersion Correction (DFT-D) for the 94 Elements H−Pu. *J. Chem. Phys.* **2010**, *132*, 154104.

(25) Ofir, Y.; Zelichenok, A.; Yitzchaik, S. 1,4;5,8-Naphthalene-Tetracarboxylic Diimide Derivatives As Model Compounds for Molecular Layer Epitaxy. *J. Mater. Chem.* **2006**, *16* (22), 2142−2149.

(26) Chen, Z.; Stepanenko, V.; Dehm, V.; Prins, P.; Siebbeles, L.; Seibt, J.; Marquetand, P.; Engel, V.; Würthner, F. Photoluminescence and Conductivity of Self-Assembled π−π Stacks of Perylene Bisimide Dyes. *Chem.—Eur. J.* **2007**, *13* (2), 436−449.

(27) Oltean, M.; Calborean, A.; Mile, G.; Vidrighin, M.; Iosin, M.; Leopold, L.; Maniu, D.; Leopold, N.; Chiş, V. Absorption spectra of PTCDI: a Combined UV-Vis and TD-DFT Study. *Spectrochim. Acta, Part A* **2012**, *97*, 703−710.

(28) Burtman, V.; Zelichonok, A.; Pakoulev, A. V. Molecular Photovoltaics in Nanoscale Dimension. *Int. J. Mol. Sci.* **2011**, *12* (1), 173−225.

(29) Pope, M.; Swenberg, C. E. *Electronic processes in organic crystals and polymers*; Oxford University Press: New York, 1999.

(30) Hunter, C. A. Quantifying Intermolecular Interactions: Guidelines for the Molecular Recognition Toolbox. *Angew. Chem., Int. Ed.* **2004**, *43* (40), 5310−5324.

(31) (a) Bełtowska-Brzezinska, M.; xuczak, T.; Holze, R. On Adsorption of Monohydric Alcohols and Diols at sp and sd Metal Electrodes. *Surf. Sci.* **1998**, *418* (1), 281−294. (b) Ikemiya, N.; Gewirth, A. A. Structure Sensitive Adsorption of DMSO on Au Surfaces. *J. Phys. Chem. B* **2000**, *104* (5), 873−877. (c) Kawasaki, H.; Yamamoto, H.; Fujimori, H.; Arakawa, R.; Iwasaki, Y.; Inada, M.

Stability of the DMF-Protected Au Nanoclusters: Photochemical, Dispersion, and Thermal Properties. *Langmuir* **2010**, *26* (8), 5926−5933.

(32) (a) Mura, M.; Silly, F.; Briggs, G.; Castell, M.; Kantorovich, L. H-Bonding Supramolecular Assemblies of PTCDI Molecules on the Au (111) Surface. *J. Phys. Chem. C* **2009**, *113* (52), 21840−21848. (b) Swarbrick, J.; Ma, J.; Theobald, J.; Oxtoby, N.; O'Shea, J.; Champness, N.; Beton, P. Square, Hexagonal, and Row Phases of PTCDA and PTCDI on Ag-Si (111) × R30°. *J. Phys. Chem. B* **2005**, *109* (24), 12167−12174. (c) Cañas Ventura, M. E.; Xiao, W.; Wasserfallen, D.; Müllen, K.; Brune, H.; Barth, J. V.; Fasel, R. Self Assembly of Periodic Bicomponent Wires and Ribbons. *Angew. Chem., Int. Ed.* **2007**, *46* (11), 1814−1818. (d) Silly, F.; Shaw, A. Q.; Castell, M. R.; Briggs, G. A Chiral Pinwheel Supramolecular Network Driven by the Assembly of PTCDI and Melamine. *Chem. Commun.* **2008**, *16*, 1907−1909.

(33) Wen, J.; Ma, J. Modulating Morphology of Thiol-Based Monolayers in Honeycomb Hydrogen-Bonded Nanoporous Templates on the Au (111) Surface: Simulations with the Modified Force Field. *J. Phys.Chem. C* **2012**, *116* (15), 8523−8534.

(34) Mura, M.; Sun, X.; Silly, F.; Jonkman, H.; Briggs, G.; Castell, M.; Kantorovich, L. Experimental and Theoretical Analysis of H-Bonded Supramolecular Assemblies of PTCDA Molecules. *Phys. Rev. B* **2010**, *81* (19), 195412.